Negative-muon spin precession in ferromagnetic iron and the hyperfine anomaly

H. Keller, R. F. Kiefl,* Hp. Baumeler, W. Kündig, and B. D. Patterson
Physik-Institut, Universität Zürich, CH-8001 Zürich, Switzerland

J. Imazato, K. Nishiyama, K. Nagamine, and T. Yamazaki
Meson Science Laboratory, Faculty of Science, University of Tokyo, Bunkyo-ku, Tokyo 113, Japan

R. I. Grynszpan
Centre National de la Recherche Scientifique, Centre d'Etudes de Chimie Métallurgique, Vitry, France
(Received 15 May 1986)

The negative-muon spin-precession technique was used to study the hyperfine field at the negative muon μ^- in ferromagnetic iron in zero applied magnetic field. In the temperature range 320–690 K the hyperfine field for μ^-Fe departs from the magnetization curve of pure iron in the same way as the hyperfine field acting upon a ^{55}Mn impurity in dilute (1.5 at.%)Mn*Fe* measured by NMR, indicating that the electronic structure of μ^-Fe is very similar to that of a Mn impurity in iron. The hyperfine anomaly Δ for μ^-Fe relative to dilute (1.5 at.%)^{55}Mn in iron is found to be $-0.9(3)\%$ and temperature independent over the temperature range investigated. The magnitude of Δ is considerably smaller than that of our value $\Delta=-2.5(4)\%$ for μ^-Ni relative to ^{59}Co in ferromagnetic nickel.

I. INTRODUCTION

Various experimental techniques such as nuclear magnetic resonance (NMR), Mössbauer spectroscopy, and time-differential perturbed angular correlation (TDPAC) have been used to study the hyperfine field (electron spin density) acting upon nuclei in ferromagnets. In addition, the positive-muon spin-rotation technique (μ^+SR) yields the electron spin density at the interstitial positive muon in ferromagnets.[1]

Much less information is available on the *radial distribution* of the electron spin density $\rho(r)$ near the nucleus. Such experiments are desirable, since they may elucidate the mechanism of core polarization.[2] The variation of $\rho(r)$ in a very small range of radii may be obtained from the hyperfine field seen by different nuclear isotopes—a consequence of the nuclear Bohr-Weisskopf effect.[3]

A wider range of radii is accessible using the negative muon μ^- as a probe. A μ^- stopped in a solid forms a muonic atom $\mu^-{}_Z X$ in which the bound μ^- behaves like a heavy electron ($m_\mu=207m_e$). The muonic radius $r_\mu=a_0 m_e/(m_\mu Z)$ is much less than the Bohr radius a_0, hence the pseudonucleus $\mu^-{}_Z X$ appears to the atomic electrons very similar to an isolated impurity nucleus of charge $Z-1$ (Ref. 4). For light elements ($Z<30$) the muonic atom $1s$-wave function extends far outside the nucleus. For example in the case of μ^-Fe, r_μ is approximately twice the nuclear radius R_0. Various properties of the muonic atoms μ^-Fe and μ^-Ni that are of interest in this paper are summarized in Table I.

If the μ^- is bound to a spinless nucleus, the pseudonucleus $\mu^-{}_Z X$ is effectively a spin-$\frac{1}{2}$ magnetic probe of $\rho(r)$. For r_μ significantly larger than R_0, the μ^- samples the electron spin density well away from the nucleus (see Fig. 1). We define $B_\mu^{\rm hf}$ as the average hyperfine field acting upon the μ^- and $B_N^{\rm hf}$ as the hyperfine field acting upon an impurity nucleus of charge $Z-1$.

Under the assumption that the muonic atom and the impurity atom occupy the same type of site in the lattice and have the same electronic structure, any difference between $B_\mu^{\rm hf}$ and $B_N^{\rm hf}$ is due to the fact that the muon samples $\rho(r)$ over a more extended region of space than the $Z-1$ nucleus (see Fig. 1). The resulting hyperfine anomaly may be defined as[4,10,11]

$$\Delta=(B_\mu^{\rm hf}-B_N^{\rm hf})/B_N^{\rm hf} . \quad (1)$$

In practice, Δ may be deduced from a combined negative-muon spin-rotation (μ^-SR) and nuclear-magnetic-resonance (NMR) experiment.[10,11]

Recently, we have observed μ^- spin precession in ferromagnetic nickel in zero applied magnetic field.[10,11] In the temperature region 20–300 K, the hyperfine anomaly

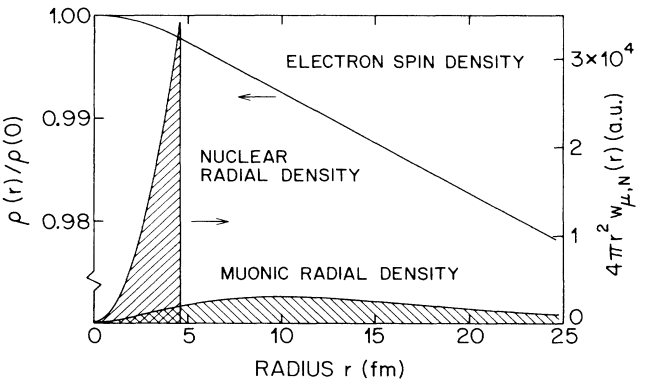

FIG. 1. Reduced electron spin density $\rho(r)/\rho(0)$ (left scale), and nuclear (Mn) and muonic (μ^-Fe) spin densities $w_{\mu,N}(r)$ (right scale) as a function of radial distance r [after Freeman *et al.* (Ref. 9)].

TABLE I. Summary of various properties of the muonic atoms μ^-Fe and μ^-Ni.

	μ^-Fe $Z=26$	μ^-Ni $Z=28$
Lifetime τ_μ (ns)[a]	206(1)	157(2)
Muon atomic radius $r_\mu=a_\mu/Z$ (fm)	9.84	9.14
$2p$-$1s$ muonic x-ray energy E_x (MeV)[b]	1.25	1.43
Recoil energy E_R (eV)	15	19
Lattice displacement energy E_D (eV)[c]	24	34.5
Relativistic correction of g factor $(g-g_0)/g_0$ (%)[d]	−0.85(5)	−0.95(5)
Gyromagnetic ratio $\gamma/2\pi$ (MHz/T)	134.38(7)	134.25(7)

[a]Eckhause *et al.* (Ref. 5).
[b]Engfer *et al.* (Ref. 6).
[c]Chadderton (Ref. 7).
[d]Interpolated values from Ford, Hughes, and Willis (Ref. 8).

for μ^-Ni relative to ^{59}Co in Ni was found to be temperature independent and equal to −2.5(4)% (Ref. 11). This is in excellent agreement with an unrestricted Dirac-Fock calculation of Freeman *et al.*[9] that yields $\Delta=(-2.3$ to $-2.7)$%, indicating that the electron spin density near the Ni nucleus decreases more rapidly than the s-electron charge density. Such behavior is a characteristic consequence of core polarization.[2,9] In this paper we report similar measurements on ferromagnetic iron. In this case the pseudonucleus μ^-Fe resembles a Mn impurity in the ferromagnetic iron host. No calculation of the hyperfine anomaly in iron has as yet been performed.

Besides the hyperfine anomaly, which is the main subject of this paper, this system has another interesting aspect. It is known from earlier NMR measurements[12] that the temperature dependence of the hyperfine field at a ^{55}Mn nucleus in dilute (1.5 at.%)Mn*Fe* departs substantially from that of the magnetization of iron. This behavior has been interpreted in terms of a simple mean-field model where the Mn impurity is treated as a localized magnetic moment.[13–15] It is interesting to investigate to what extent the average hyperfine field in μ^-Fe exhibits the same temperature behavior, since any differences would indicate a change in the electronic structure of μ^-Fe relative to a Mn impurity.

II. HYPERFINE ANOMALY

In the framework of the extended Bohr-Weisskopf model[4] the hyperfine anomaly Δ in Eq. (1) may be written in the form

$$\Delta=\varepsilon_\mu-\varepsilon_N \tag{2a}$$

with

$$\varepsilon_{\mu,N}=\int 4\pi r^2 w_{\mu,N}(r)[\rho(r)/\rho(0)]dr-1\ , \tag{2b}$$

where ε_μ (ε_N) is the muonic (nuclear) hyperfine anomaly relative to a hypothetical pointlike nucleus. The quantities $w_\mu(r)$, $w_N(r)$, and $\rho(r)$ are the muon, the nuclear, and the electron spin density, respectively. For a pointlike probe $w(r)$ is a δ function, and ε is zero by definition. One can estimate ε_μ and ε_N in Eq. (2) by making the following assumptions (see Fig. 1). (i) $\rho(r)$ as well as $w_\mu(r)$ in Eq. (2b) are represented by hydrogenlike $1s$-wave functions. This is valid for atoms ($Z<30$) where one can neglect the finite nuclear size relative to the muonic and electronic radii. (ii) The nuclear spin density $w_N(r)$ is constant inside the nuclear sphere and zero outside. (iii) $\rho(r)$ has the nonrelativistic form

$$\rho(r)=\rho(0)[1-Zr^2/(a_0R_0)]$$

for $r<R_0$. With these assumptions an evaluation of the integrals in Eq. (2b) yields[4]

$$\varepsilon_\mu^0=-3m_e/m_\mu=-1.45\%\ , \tag{3a}$$

$$\varepsilon_N^0=-\tfrac{3}{5}(R_0/a_0)Z\simeq-1.4\times10^{-5}ZA^{1/3}\ . \tag{3b}$$

Note that the muonic anomaly ε_μ is independent of Z when the finite nuclear size is neglected. For a Mn nucleus ($Z=25$) the above estimate of the nuclear hyperfine anomaly [Eq. (3b)] gives $\varepsilon_N^0=-0.13\%$ (nuclear Bohr-Weisskopf effect). As expected for light elements ($Z<30$), $|\varepsilon_\mu^0|$ is much larger than $|\varepsilon_N^0|$, because the muonic atom $\mu^-{}_ZX$ probes the electron spin density at distances much further away from the origin than does

the nucleus of charge $Z-1$. For μ^-Fe relative to Mn our simple estimate [Eq. (3)] leads to a hyperfine anomaly of

$$\Delta=\varepsilon_\mu^0-\varepsilon_N^0=-1.3\% \ . \tag{4}$$

Note that this value is obtained under the condition that the electron spin and the electron charge density are proportional to one another. This is an unwarranted assumption in the case of a ferromagnetic transition metal where the mechanism of core polarization plays an essential role.[2,9] The magnetic $3d$ electrons polarize the inner core s electrons due to the attractive exchange interaction between electrons of parallel spins leading to a negative spin density at (near) the nucleus which decreases with radial distance more steeply than the charge density. Core polarization is primarily responsible for the difference between our simple estimate for Δ [Eq. (4)] and the calculated result of Freeman *et al.*[9] for μ^-Ni relative to Co.

III. EXPERIMENTAL DETAILS

The experiment was performed at the Swiss Institute for Nuclear Research (SIN) with an 80%-polarized negative-muon beam with a momentum of 125 MeV/c.

The high-purity iron sample ($19\times18\times7$ mm^3), consisting of seven single-crystal plates, was mounted in an oven containing a helium exchange gas in order to maintain a uniform temperature over the sample. Measurements were performed in the temperature range 320—690 K, and the sample temperature was measured and controlled using two Ni-Cr—Ni thermocouples. The relative long-term (24-h) temperature stability was ±0.1 K at 320 K and ±1 K at 690 K, respectively (Table II).

In order to resolve the rather high μ^- precession frequencies of μ^-Fe (2.5 GHz at 320 K), a high-timing resolution μSR apparatus[16] was used (see Fig. 2). The incoming muons were collimated and degraded in $(CH_2)_n$ before stopping in the sample. A stopped muon and the subsequent electron from μ^- decay were defined by the coincidences $BM_t\bar{F}$ and $FE_t\bar{M}_t$, respectively, where B, M_t, F, and E_t are plastic scintillation detectors. In order to achieve the required timing resolution, fast scintillator material (Nuclear Enterprises NE111), fast photomultipliers (Philips XP2020), and differential constant fraction discriminators were used for the detectors M_t and E_t. An estimate of the timing resolution $\Delta\tau$ of the detector system was made from the dependence of the observed precession amplitudes A on frequency (see Table II). Assuming a Gaussian time-resolution function, the experimental amplitude is given by[16]

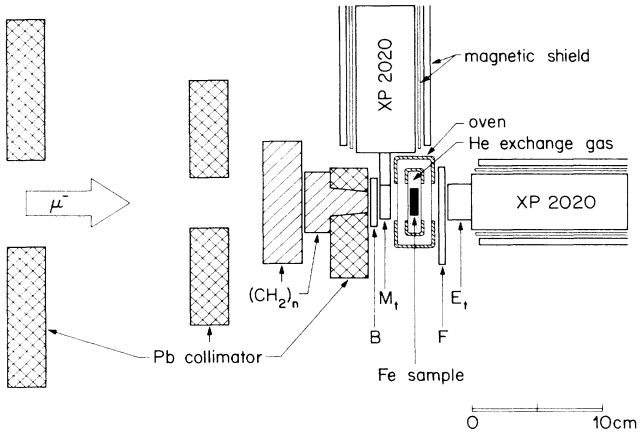

FIG. 2. Diagram of the high-timing-resolution μ^-SR apparatus. B, M_t, F, and E_t denote plastic scintillation counters, where M_t and E_t are the time-defining muon and electron counters, respectively.

$$A=A_0\exp[-(\pi\nu_\mu\Delta\tau)^2/(4\ln2)] \ , \tag{5}$$

where A_0 is the intial amplitude and ν_μ is the Larmor precession frequency. A fit of our data to Eq. (5) yields a timing resolution $\Delta\tau=242(29)$ ps and $A_0=1.05(20)\%$.

The time spectrum was measured with a time-to-amplitude converter (TAC). The TAC signals were digitized by an analog-to-digital converter (ADC) and stored in a 8192 channel time histogram of an on-line computer. In each spectrum, $(10-13)\times10^6$ events were accumulated with a typical event rate of 150/s. The time scale was periodically calibrated with a precision quartz clock.

The general form of a μSR time spectrum consists of an exponential decay modulated by the precession pattern of the muon spin polarization in the local magnetic field:

$$N(t)=N_0\exp(-t/\tau_\mu) \times[1+A\exp(-\lambda t)\cos(2\pi\nu_\mu t+\Phi)]+B \ . \tag{6}$$

Here N_0 is a normalization factor, τ_μ is the lifetime of the μ^-, A is the precession amplitude, λ is the muon relaxation rate, Φ is the initial phase, and B is a time-independent background term. The μ^- lifetime in a muonic atom is considerably shorter than the free μ^- life-

TABLE II. Summary of μSR parameters for μ^-Fe. ν_μ is the muon precession frequency, A is the precession amplitude, λ is the muon relaxation rate, and τ_μ is the effective muon lifetime [cf. Eq. (6)].

Temperature (K)	ν_μ (MHz)	A (%)	λ (μs^{-1})	τ_μ (ns)
322.9(1)	2459.0(11)	0.27(12)	1.5(27)	193.2(8)
395.4(2)	2218.1(12)	0.37(13)	3.6(25)	190.9(9)
495.7(3)	1905.8(6)	0.66(20)	7.0(33)	190.8(9)
590.4(4)	1649.4(8)	0.58(12)	3.7(15)	192.4(8)
638.0(6)	1539.4(8)	0.62(23)	7.1(37)	191.4(9)
691.5(10)	1425.5(7)	0.67(19)	7.4(32)	191.4(8)

TABLE III. Comparison of μ^-Fe spin rotation and ^{55}Mn NMR in (1.5 at.%)Mn*Fe*. The hyperfine anomaly is determined by $\Delta=(B_\mu-B_N)/(B_N-B_L)$, where B_N is the nuclear local field, B_μ is the muonic local field, and B_L is the Lorentz field.

Temperature (K)	μ^-Fe B_μ (T)[a]	^{55}Mn*Fe* B_N (T)[b]	B_L (T)[c]	Δ (%)
322.9(1)	−18.298(12)	−18.414(50)	0.717(2)	−0.6(3)
322.9(1)		−18.377(50)[d]		[−0.4(3)][e]
395.4(2)	−16.505(12)	−16.609(50)	0.710(2)	−0.6(3)
495.7(3)	−14.182(8)	−14.291(50)	0.694(2)	−0.7(3)
590.4(4)	−12.273(9)	−12.430(50)	0.673(2)	−1.2(4)
638.0(6)	−11.455(8)	−11.604(50)	0.660(2)	−1.2(4)
691.5(10)	−10.607(8)	−10.720(50)	0.643(2)	−1.0(4)

[a] $B_\mu=\nu_\mu/[134.38(7)$ MHz/T], see Tables I and II.
[b] Interpolated values from Koi *et al.* (Ref. 12) with $B_N=\nu_N/[10.529(4)$ MHz/T] (Ref. 18).
[c] Interpolated values of iron magnetization data from Crangle and Goodman (Ref. 19).
[d] Interpolated value for (1 at.%)Mn*Fe* from Yamagata (Ref. 20).
[e] Value for (1 at.%)Mn*Fe*.

time (2.2 μs), due to the fact that a bound μ^- may be captured by the nucleus (Table I).[5]

In the present work the measured μSR time spectra were analyzed in two different ways. (i) The time spectra were fitted directly to Eq. (6) with N_0, τ_μ, A, λ, ν_μ, Φ, and B as free parameters, including the cyclotron rf frequency (50 MHz) and its harmonics. (ii) The complex Fourier transforms of the time spectra were fitted to the Fourier transforms of Eq. (6) keeping the muon lifetime $\tau_\mu=192$ ns (Table II) fixed. A typical frequency spectrum of μ^-Fe is shown in Fig. 3. Identical results were obtained with both fitting procedures. The fitted parameters obtained in the time interval 26—328 ns are listed in Table II. Note that our value for the muon lifetime $\tau_\mu=192(1)$ ns is about 7% smaller than the experimental value of 206(1) ns for Fe given in the literature (Table I). This reduction of τ_μ may be understood assuming that about $\frac{1}{3}$ of the incoming muons were stopped in the copper sample holder, since the μ^-Cu lifetime [163.6(8) ns (Ref. 5)] is smaller than for μ^-Fe.

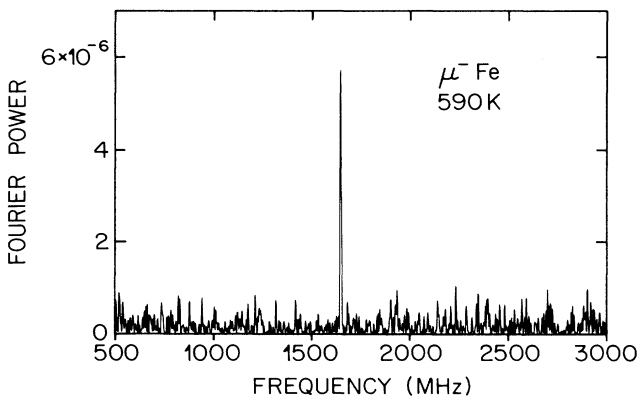

FIG. 3. Typical μ^-SR frequency spectrum of single-crystal iron taken at 590 K.

The initial μ^- precession amplitude A_0 is determined by several factors:[11] (1) the beam polarization, (2) the fraction of muons stopping in the sample, (3) the depolarization during muonic atom formation and cascade,[17] (4) the fraction of domains magnetized perpendicular to the muon polarization, and (5) the asymmetry of μ^- decay and the finite solid angle of the electron telescope. The contribution of all factors except (3) was determined to be 7.1(5)% by measuring the μ^+ precession amplitude. For a spinless nucleus, factor (3) is roughly 15% (Ref. 17). Therefore, the expected μ^- precession amplitude is 1.1(1)%, which is in agreement with the experimental value $A_0=1.05(20)$%, corrected for finite timing resolution.

The local magnetic field B_μ at the muon in μ^-Fe was determined from the measured precession frequencies ν_μ (Table II), taking account of the relativistic correction of the bound muon g factor relative to the free value g_0: $(g-g_0)/g_0=-0.85(5)$% (Table I).[8] The sign of B_μ is assumed to be negative since the internal field at Mn in Mn*Fe* is known to be negative from NMR on oriented ^{52}Mn in Fe (Ref. 18). This is a consequence of core polarization[2] of the inner shell electrons by the polarized $3d$ electrons. The resulting local magnetic fields $B_\mu(T)$ are summarized in Table III.

IV. RESULTS

The temperature dependence of the local (hyperfine) field at the nucleus of an impurity atom in a ferromagnetic host usually follows closely the magnetization of the bulk host. However, for certain magnetic impurity atoms such as Mn in iron, substantial deviations from this behavior are observed. The local magnetic field B_N at ^{55}Mn in dilute ferromagnetic (1.5 at.%)Mn*Fe* has previously been investigated by means of NMR by several groups.[12,21,22] As shown in Fig. 4, the temperature dependence of B_N departs considerably from that of the iron magnetization curve.

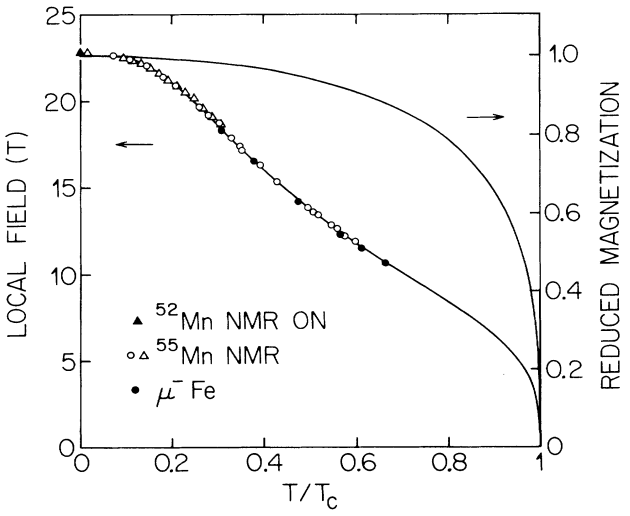

FIG. 4. Magnitude of local field in iron as a function of reduced temperature $T/T_c(T_c=1043$ K). Solid triangle: Data for ^{52}Mn*Fe* (dilute limit) obtained with NMR on oriented ^{52}Mn nuclei (NMR ON) from Ref. 18. Open circles and open triangles: ^{55}Mn NMR data for (1.5 at.%)^{55}Mn*Fe* from Refs. 12 and 22, respectively. Solid circles: μ^-Fe data for iron. The solid line corresponds to a fit to the NMR data of ^{55}Mn*Fe* to the simple mean-field model described in the text. For comparison the reduced magnetization curve of pure iron is also shown (right scale).

This anomalous behavior was first interpreted by Jaccarino *et al.*[13] in terms of a simple mean-field model where the Mn impurity is treated as a localized magnetic moment. An extended version of this model has been proposed by Low[14] and Shirley *et al.* (Ref. 15). In this work we adopt the mean-field model of Shirley *et al.* where the local field B at the nucleus (muon) is the sum of two contributions:

$$B(T)=B_{\rm LM}(T)+B_C(T)\ . \tag{7}$$

Here $B_{\rm LM}(T)$ is the field of the localized Mn moment, and $B_C(T)$ is a contribution from the polarized conduction electrons. The localized magnetic moment of spin J is oriented in the host-impurity exchange field $B_{\rm ex}(T)$, and thus $B_{\rm LM}(T)$ is proportional to the Brillouin function $\tilde{B}_J(y)$ with $y=g\mu_B JB_{\rm ex}(T)/(k_BT)$. The conduction-electron contribution $B_C(T)$ as well as the exchange field $B_{\rm ex}(T)$ are assumed to follow the reduced lattice magnetization $\sigma(T)$. Therefore we may write for Eq. (7)

$$B(T)=B_{\rm LM}(0)\tilde{B}_J(y)+B_C(0)\sigma(T)\ , \tag{8a}$$

with

$$y=\xi\sigma(T)T_c/T\ . \tag{8b}$$

Here the dimensionless parameter $\xi=g\mu_B JB_{\rm ex}(0)/(k_BT_c)$ is a measure of the host-impurity exchange interaction. It is conventional to express Eq. (8) in the form

$$B(T)=B(0)[f\tilde{B}_J(y)+(1-f)\sigma(T)]\ , \tag{9}$$

where $f=B_{\rm LM}(0)/B(0)$. The ^{55}Mn NMR data[12,22] for (1.5 at%)Mn*Fe* were fitted to Eq. (9) with $B(0)$, ξ, and f as adjustable parameters and with the Curie temperature $T_c=1043$ K fixed. Experimental values for the reduced magnetization $\sigma(T)$ of pure iron were taken from Ref. 19. For $\frac{1}{2}<J<2$ almost identical fits were obtained, and thus an exact determination of J with this fitting procedure was not possible.[15] The best fit was obtained for $J=\frac{3}{2}$ with $B(0)=-22.69(3)$ T, $\xi=0.700(8)$, and $f=0.99(1)$ as shown by the solid curve in Fig. 4. These results are in agreement with the previous results of Ref. 15 ($\xi=0.711$, $f=0.97$). Our fitted value $B(0)=-22.69(3)$ T is somewhat larger than the experimental value $B(0)=-22.803(18)$ T for ^{52}Mn*Fe* measured at 10 mK by means of NMR on oriented ^{52}Mn (Ref. 18 and Fig. 4). The fact that $f\simeq 1$ indicates that the conduction-electron contribution B_C in Eqs. (7) and (9) is very small, in agreement with the mean-field model of Jaccarino *et al.*,[13] where $f=1$.

The temperature dependence of the local magnetic field B_μ at the muon in μ^-Fe (Table III) is shown in Fig. 4. Note that in the temperature range investigated B_μ exhibits approximately the same temperature dependence as the local field B_N acting upon a Mn nucleus in dilute Mn*Fe*. This observation clearly demonstrates that the electronic structure of μ^-Fe is indeed very similar to that of a Mn impurity in the iron host.

In zero external field the hyperfine field $B^{\rm hf}_{\mu,N}$ at the muon and the nucleus, respectively, is given by

$$B^{\rm hf}_{\mu,N}=B_{\mu,N}-B_L\ , \tag{10}$$

where $B_{\mu,N}$ is the local field, and $B_L=(4\pi/3)M_s$ is the Lorentz field. Assuming that B_L is the same for μ^-Fe and Mn in the iron host, one may write for the hyperfine anomaly defined in Eq. (1):

$$\Delta=(B_\mu-B_N)/(B_N-B_L)\ . \tag{11}$$

For the temperatures investigated B_N was determined by interpolating the NMR data of Ref. 12 with a polynomial of degree four. The Lorentz field $B_L=(4\pi/3)M_s$ was calculated using known experimental values for the saturation magnetization M_s of pure iron.[19] With these assumptions the hyperfine anomaly was determined according to Eq. (11). The resulting values of Δ are summarized in Table (III). The hyperfine anomaly for μ^-Fe relative to Mn in Fe is found to be approximately *temperature independent* in the range 320–690 K with an average value of $\Delta=-0.9(3)\%$. This value of Δ is in magnitude considerably smaller than that of $\Delta=-2.5(4)\%$ obtained for μ^-Ni relative to Co in ferromagnetic nickel,[11] but surprisingly, is in fair agreement with our simple estimate of $\Delta=-1.3\%$ [Eq. (4)] where the effect of core polarization is neglected.

V. DISCUSSION

The most interesting result of this work is the fact that a muonic atom μ^-Fe ($Z=26$) exhibits approximately the same magnetic properties as a Mn ($Z=25$) impurity atom (localized magnetic moment) in a ferromagnetic iron host, implying that the electronic structures of these two species are very similar.

A few comments should be made concerning the rather small experimental value of the absolute hyperfine anomaly for μ^-Fe relative to Mn compared to that for μ^-Ni relative to Co.

(1) During the cascade into the $1s$ ground state the muonic atom may be ejected from its lattice site due to emission of an x ray.[11] For μ^-Fe the maximum x-ray energy ($2p$-$1s$ transition) is 1.25 MeV corresponding to a recoil energy of $E_R = 15$ eV. Since E_R is smaller than the lattice displacement energy $E_D = 24$ eV (Table I), a large fraction of μ^-Fe should occupy undistorted lattice sites. This is also evident from the fact that the precession signals are rather narrow and have the expected amplitudes (Fig. 3). For μ^-Ni the situation is quite similar, as shown in Table I (Ref. 11). Therefore, we conclude that the difference between the observed hyperfine anomalies for μ^-Fe relative to Mn and μ^-Ni relative to Co is most likely not due to lattice displacement. Note that in a previous experiment a rather large hyperfine anomaly of $-36(5)\%$ was observed for μ^-Pd relative to Rh at 11 K (Ref. 4) which disagrees with the theoretical value of -5% obtained from unrestricted Dirac-Fock theory.[23,9] For μ^-Pd the x-ray energy is 3.1 MeV (Ref. 6), implying a recoil energy of 48 eV which is 3 times larger than for μ^-Ni and μ^-Fe. Mallow *et al.*[23] have thus suggested that the large hyperfine anomaly of -36% is probably due to interstitial μ^-Pd.

(2) In a μSR experiment only one μ^-Fe "impurity atom" is present in the sample at a given instant of time (dilute limit). However, our results are compared with NMR data[12,22] for (1.5 at.%)^{55}Mn*Fe* which may not represent the dilute limit.[24] Moreover, these NMR data were taken in zero external field where the resonances from Mn nuclei in domain walls dominate.[11] These hyperfine fields may differ from those obtained from domains, with which our μ^-Fe data actually should be compared. Hagn *et al.*[18] have precisely measured the local field B_N at ^{52}Mn in Fe as a function of external field by means of NMR on oriented ^{52}Mn. By extrapolating these data to zero field they find $B_N(10\text{ mK}) = -22.803(18)$ T (dilute limit). Yamagata and Matsumura[22] have determined $B_N(17\text{ K}) = -22.77(2)$ T for (1.5 at.%)Mn*Fe* in zero applied field. An extrapolation of this value to 0 K yields $B_N(0\text{ K}) = -22.78(2)$ T. This would imply only a small correction of $-0.1(1)\%$ in the hyperfine anomaly for μ^-Fe relative to (1.5 at.%)Mn*Fe* at 0 K.

In conclusion, we have measured the hyperfine anomaly for μ^-Fe relative to (1.5 at.%)Mn*Fe* to be $\Delta = -0.9(3)\%$. The effect is significantly smaller than expected if core polarization plays a similar role in μ^-Fe relative to Mn as in μ^-Ni relative to Co. The reason for the small magnitude of Δ is not known.

In order to obtain a more reliable value for the anomaly, the experiment should be performed at low temperatures (4 K). In this case the μSR results could be compared directly with the NMR data[18] on oriented ^{52}Mn in iron (dilute limit, no domain-wall resonance). Such an experiment, however, is a rather difficult task, since a very high-timing resolution is required to observe muon precession frequencies above 3 GHz. It would be highly desirable to have a theoretical value for the anomaly from an unrestricted Dirac-Fock calculation[9,23] with which the experimental results could be compared.

ACKNOWLEDGMENTS

The authors would like to thank Dr. H. Yamagata (Kochi University, Japan) for kindly providing us with NMR data of Mn*Fe*. This work was supported by the Swiss National Science Foundation, by the Swiss Institute for Nuclear Research (SIN), and by a Grant-in-Aid from the Japanese Ministry of Education, Culture, and Science. One of us (R.F.K.) would like to thank the National Research Council of Canada for additional support.

*Present address: TRIUMF, 4004 Wesbrook Mall, Vancouver, B.C., Canada V6T 2A3.

[1]See, e.g., A. B. Denison, H. Graf, W. Kündig, and P. F. Meier, Helv. Phys. Acta **52**, 460 (1979).

[2]A. J. Freeman and R. E. Watson, in *Magnetism*, edited by G. T. Rado and H. Suhl (Academic, New York, 1965), Vol. IIA, Chap. 4.

[3]A. Bohr and V. F. Weisskopf, Phys. Rev. **77**, 94 (1950); H. H. Stroke, R. J. Blin-Stoyle, and V. Jaccarino, *ibid.* **123**, 1326 (1961).

[4]T. Yamazaki, R. S. Hayano, Y. Kuno, J. Imazato, K. Nagamine, S. E. Kohn, and C. Y. Huang, Phys. Rev. Lett. **42**, 1241 (1979); T. Yamazaki, Hyperfine Interact. **8**, 463 (1981).

[5]M. Eckhause, R. T. Siegel, R. E. Welsh, and T. A. Filippas, Nucl. Phys. **81**, 575 (1966).

[6]R. Engfer, H. Schneuwly, J. L. Vuilleumier, H. K. Walter, and A. Zehnder, At. Data Nucl. Data Tables **14**, 509 (1974).

[7]L. T. Chadderton, *Radiation Damage in Crystals* (Methuen, London, 1965).

[8]K. W. Ford, V. W. Hughes, and J. G. Wills, Phys. Rev. Lett. **7**, 134 (1961); Phys. Rev. **129**, 194 (1963).

[9]A. J. Freeman, J. V. Mallow, J. P. Desclaux, and M. Weinert, Hyperfine Interact. **17-19**, 865 (1984).

[10]J. Imazato, K. Nagamine, T. Yamazaki, B. D. Patterson, E. Holzschuh, and R. F. Kiefl, Hyperfine Interact. **17-19**, 857 (1984).

[11]J. Imazato, K. Nagamine, T. Yamazaki, B. D. Patterson, E. Holzschuh, and R. F. Kiefl, Phys. Rev. Lett. **53**, 1849 (1984).

[12]Y. Koi, A. Tsujimura, and T. Hihara, J. Phys. Soc. Jpn. **19**, 1493 (1964).

[13]V. Jaccarino, L. R. Walker, and G. K. Wertheim, Phys. Rev. Lett. **13**, 752 (1964).

[14]G. G. Low, Phys. Lett. **21**, 497 (1966).

[15]D. A. Shirley, S. S. Rosenblum, and E. Matthias, Phys. Rev. **170**, 363 (1968).

[16]E. Holzschuh, W. Kündig, and B. D. Patterson, Helv. Phys. Acta. **54**, 552 (1981); E. Holzschuh, Phys. Rev. B **27**, 102 (1983).

[17]R. A. Mann and M. E. Rose, Phys. Rev. **121**, 293 (1961).

[18]E. Hagn, E. Zech, and G. Eska, J. Phys. F **12**, 1475 (1982).

[19]J. Crangle and G. M. Goodman, Proc. R. Soc. London, Ser. A **321**, 477 (1971).

[20]H. Yamagata (private communication).
[21]M. Rubinstein, G. H. Strauss, and J. Dweck, Phys. Rev. Lett. **17**, 1001 (1966).
[22]H. Yamagata and M. Matsumura, J. Magn. Magn. Mater. **31-34**, 65 (1983).
[23]J. V. Mallow, J. P. Desclaux, A. J. Freeman, and M. Weinert, Hyperfine Interact. **8**, 455 (1981).
[24]Note, however, that at 323 K the values of Δ for (1.5 at.%) and (1 at.%)Mn*Fe* agree within the experimental error (Table III).